Construction and Building Materials 116 (2016) 413–421

Contents lists available at ScienceDirect

Construction and Building Materials

journal homepage: www.elsevier.com/locate/conbuildmat

# Evaluation of axle load increasing on a monumental masonry arch bridge based on field load testing

Shervan Ataei *, Meysam Jahangiri Alikamar, Vahid Kazemiashtiani

*School of Railway Engineering, Iran University of Science and Technology, Tehran, Iran*

## HIGHLIGHTS

- Capacity assessment of a 80 years old masonry arch bridge.
- Performing the displacement measurement of the main span with the length of 40 m and height of 30 m with the precision of 0.01 mm.
- Finite element model updating based on the displacement measurement results.
- Computing the dynamic impact factor based on the measurement results.
- Assessment the potential of axle load increasing based on the updated finite element model and the RING software and comparing their results.

## ARTICLE INFO

*Article history:*
Received 28 October 2015
Received in revised form 17 April 2016
Accepted 26 April 2016
Available online 9 May 2016

*Keywords:*
Axle load increasing
Masonry arch bridge
Field testing
Finite element model updating
Four plastic hinges mechanism

## ABSTRACT

The importance and long serviceability period of a curved-in-plan masonry arch bridge, and the demand for allowable axle load increasing from 200 to 250 kN, convinced the authors to thoroughly assess the structure under the current standard loading conditions. Through the process of this research, the structure was modeled by taking advantage of the finite element method which accompanied by the model calibration using the obtained results of a predesigned field test, in which the precision of displacement measurement at the middle of main arch (with the height of 30 m from the riverbed) was 0.01 mm. By considering the dynamic impact factor resulted from the field test, the four plastic hinges mechanism and the serviceability limit state have been applied. Consequently, the ultimate adequacy factors of the bridge were resulted by the calibrated finite element model and the RING software. A reasonable agreement between the results was observed that assured the serviceability of the bridge for the current loading condition and even higher up to 250 kN.



## 1. Introduction

Masonry arch bridges with inherent special architecture are among the historic structures in railway engineering. There are about 3000 masonry arch bridges in Iran which are still in service as the railway infrastructures. In current condition, due to the long serviceability period up to a century and the demand for allowable axle load increasing, the capacity assessment of these types of bridges seems vital. Based on the different types of materials, these types of structures could be divided to the ones constructed by brick, stone or unreinforced concrete. In the recent decades, the number of researches carried out in the field of capacity assessment of masonry arch bridges, are enormous; most of which tried analytical and numerical methods [1]. To perform capacity estimation of the bridges in different accuracy and complexity levels, one could refer to the MEXE, Limit Analysis-Equilibrium, Limit Analysis-Mechanism, and verified 2&3 dimensional Finite Element Modeling methods with the field testing [2,3].

Atamturktur and Boothby [4] carried out a research regarding the behavior of such bridges with the spans of 3–12 m. The 3D finite element models of the structures have been calibrated by the results of the field testing, modal analysis and implementation of a concentrated load. According to the obtained results, the authors recommended some points referring to the finite element modeling, two of which are the model mesh creation, and the material properties allocation. In 2001, Frýba and Pirner [5] performed a stress analysis project for the road bridges. Considering both static and dynamic loads, the researchers evaluated the stress level in the structures. In the research, the results of the analysis have been exploited to estimate the fatigue life time of the studied bridges. In 2004, Marefat et al. [6] conducted an experiment in

* Corresponding author at: School of Railway Engineering, Iran University of Science and Technology, P.O. Box 16846-13114, Tehran, Iran.
*E-mail address:* ataei@iust.ac.ir (S. Ataei).

http://dx.doi.org/10.1016/j.conbuildmat.2016.04.126
0950-0618/

which a mass-concrete arch bridge was loaded near the failure point. Although the load increment had affected the growing of the appeared crack in the keystone, there was a slight reduction in the bridge stiffness. The amount of the static load resisted by the bridge was 6000 kN. In 2005, Robert-Nicoud et al. [7] proposed a method for model validation based on the structural conditions such as the support and the material status. According to the reported results, an algorithm for the arch bridges model validation was proposed. Caglayan et al. [8] presented the behavioral characteristics of a masonry arch bridge due to the static and dynamic loads in 2011. The researchers applied the field test findings of a bridge with 210 m length for calibration of the finite element model. The authors finally assessed the bridge capacity with the load rating factor, which is one of the key parameters that define the status of a bridge and its response to the various loads.

In 2013, Carr et al. [9] focused on the first hinge formation for evaluating the historic masonry arch bridges. The researches obtained the capacity of such bridges for the considered live loads and presented a safe loading margin to prevent the plastic hinge formation. The results for a specific bridge indicate that the required live load for plastic hinge formation is about 50 percent of the ultimate loading resisted by the bridge which had been modeled in the Ring.3. In 2014, Reccia et al. [10] considered the moving load problem in the modeling and analysis of a railway masonry arch bridge. The authors created a detailed 3D model of a masonry arch bridge in both commercial and noncommercial finite element software. The results show the adequacy of the bridge for the examined moving loads. The work also discusses the stiffness ratio of the materials on the bridge responses in both software.

Plastic analysis method is another way of the assessment of the masonry arch bridges. This approach is divided to the four plastic hinges and the hard blocks methods. The plastic analysis was developed for arches by Heyman [11]. In 1988, Harvey [12] defined the four plastic hinges as the method in which the arch would be healthy otherwise the fourth hinge forms.

In 2015, Costa et al. [13] were carried out a vibration field testing to evaluate the modal characteristics of a single span masonry arch railway bridge. Based on the obtained results, the finite element model of the bridge was updated. In order to considering the true behavior of the material and the modeling of which, some experiments were conducted on the bridge materials. The researchers made it possible to update the finite element modeling without performing any filed load testing.

In 2006, Cavicchi and Gambarotta [14] created a 2 dimensional finite element model of a masonry arch bridge to perform the capacity assessment. Failure mechanism and bridge capacity were studied in this research. The span length of the studied bridge was 6.55 m while the arch rise was 1.428 m. Regarding the loading issue in the field testing, a concentrated load at the quarter point of span of the bridge was implemented. Consequently, the results indicated that the loading value at the failure point was about 288 kN.

In 2003, the behavior of a masonry arch bridge with stone blocks (Bargower Bridge) was evaluated based on the mechanism method by Ng and Failfield [15]. The applicability of this method is in the condition in which all implemented loads and their locations are clearly identified. The researchers introduced a new mechanism method which consists of deflection-dependent pressure updating algorithm. The results of the study illustrated the significant effects of the arch displacement on the bridge loading capacity.

In 2008, Brencich and Sabia [16], created a 3 dimensional finite element model of a masonry arch bridge (Tanaro, constructed in 1866) with 18 spans and evaluated the bridge under service loading. The authors also considered the results of the modal frequencies which had been obtained from the field testing to verify the outputs of the model. The results of the research indicated that the investigation of a segment of the bridge does not represent the true behavior of the bridge and is not satisfactory for the modal evaluation of the entire bridge.

## 2. Research methodology

In this research, for considering the possibility of allowable axle load increasing from 200 to 250 kN, the assessment of a masonry arch bridge located in the Zagros railway region (Iran) has been conducted for the current standard loading (Fig. 16).

The research methodology is illustrated in Fig. 1. As it can be observed, in the first step, the geometrical and mechanical properties of the bridge are determined precisely. The geometrical properties are extracted from the structural as-built plans. For obtaining the accurate properties of materials, some experimentation results of the mechanics of materials for different segments of the bridge are taken. The obtained properties lead to the creation of an accurate 3 dimensional finite element model which is performed in ABAQUS software [17]. The constructed model is calibrated by taking advantage of the results of the dynamic field load testing and specifically through the displacements control. Then, the updated model is used to evaluate the bridge load capacity.

There are a number of parameters which are obtained in the current research:

1) Ultimate load calculation with the updated FEM - the four plastic hinges mechanism – the partial factors for load and material have been ignored.
2) Ultimate load calculation with the RING [18] software - the partial factors for load and material have been ignored.
3) The first and the second items above by considering the partial factors for load and material, and also considering the impact factor.
4) Controlling the bridge in serviceability limit state with the updated FEM.

## 3. The bridge properties

As mentioned before, the studied structure, the 80 years old Saleh-Hamid Bridge, located near the Tange 7 train station in Lorestan province, Iran, has 200 m length with the maximum of 30.5 m height. From the plan view, the bridge has two curves with the radius of 340 m at the ends and a curve with the radius of 490 m in the middle. There is no reinforcement used in the bridge construction and all material types for piers, foundation and arches are masonry. Moreover, low strength concrete plays the role of infill. Superstructure consists of ballast materials, Rail (U33), and steel sleepers. Figs. 2 and 3 show the bridge view and longitudinal profile (side view), respectively.

Mechanical properties of the materials have been extracted through coring and experimentation. Geometrical and material properties can be observed in Tables 1 and 2 respectively.

As it can be observed from the table, the seventh arch with the length of 40 m is the main arch.

## 4. Field testing and instrumentation

To perform the load testing of the Saleh-Hamid Bridge, multiple sensors have been used. DCDT (Deflected Cantilever Displacement Transducer) and Accelerometers are the types of the exploited sensors. In Fig. 4, the locations of the sensors are illustrated.

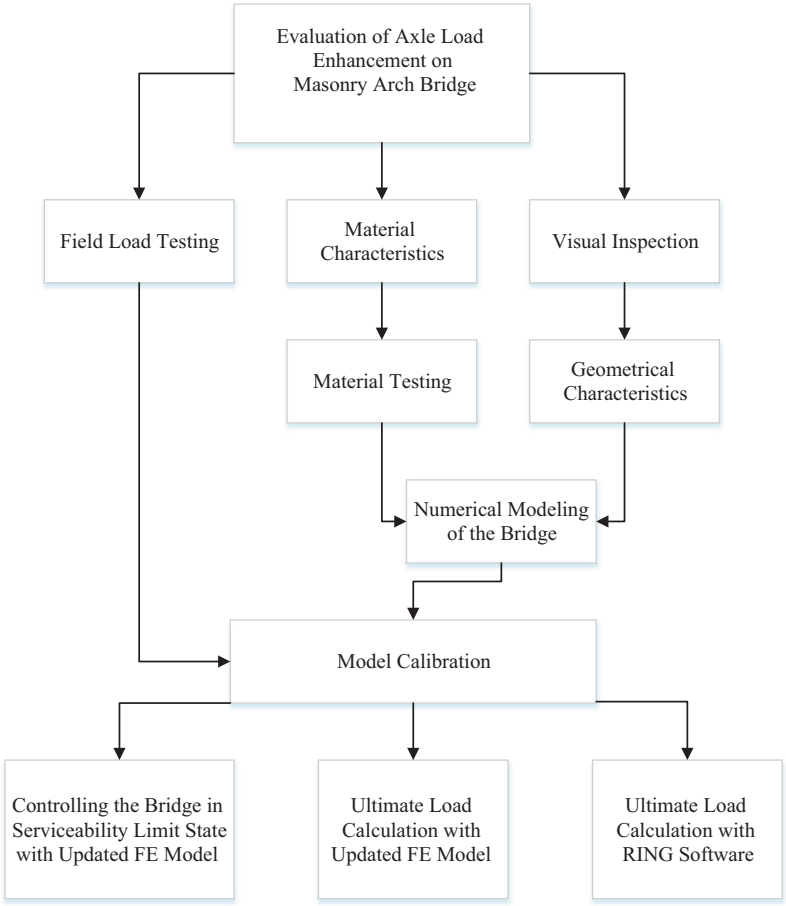


**Fig. 1.** Research methodology.

**Fig. 2.** Overall view of the bridge.

### 4.1. Displacement measurement sensor (DCDT) installation

In this research project, the vertical displacement of the bridge has been measured. Treatment of the common LVDT (linear variable differential transformer) sensors was hard to achieve, since there were some limitations in the field such as the height (about 30 m) and framework installation. The dynamic measurement of displacement requires precise (minimum 0.01 mm) evaluation. The measurement is based on considering the level changes of the structure to a fixed point beneath.

Consequently, the DCDT sensors were installed which enable experts to measure the dynamic vertical displacement of the outer clamp pulled inside as a results of the beam (cantilever inside the instrument) tension force. Therefore, it is sufficient to connect the sensor and clamp through a wire.

The DCDT sensors have the capability of measuring displacement in the range of 25 mm and 10 μm precisions. Appropriate stiffness of the cantilever shaped element which has been positioned in the sensor causes the in shape position of all involved

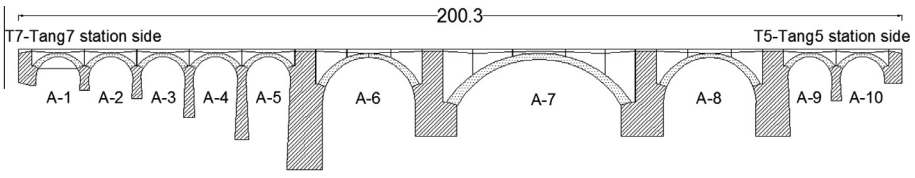


**Fig. 3.** Bridge side view.

**Table 1**
Geometrical properties of the bridge.

| Arch Number | Span Length (m) | Keystone Depth (m) | Skewback Width (m) | Bridge Width (m) | Pier Height (m) | Arch rise (m) | Pier thickness (m) |
|---|---|---|---|---|---|---|---|
| 1 | 10 | 0.80 | 1.32 | 4.5 | 9.3 | 2.76 | 4.5 |
| 2 | 10 | 0.80 | 1.32 | 4.5 | 10.3 | 2.76 | 4.5 |
| 3 | 10 | 0.80 | 1.32 | 4.5 | 13.425 | 2.76 | 4.5 |
| 4 | 10 | 0.80 | 1.32 | 4.5 | 18.05 | 2.76 | 4.5 |
| 5 | 10 | 0.80 | 1.32 | 4.5 | 23.9 | 2.76 | 4.5 |
| 6 | 21 | 1.00 | 1.90 | 4.6 | 23.51 | 6.69 | 4.6 |
| 7 (Main Arch) | 40 | 1.40 | 2.50 | 5 | 19.76 | 10.75 | 5.86 |
| 8 | 21 | 1.00 | 1.90 | 4.6 | 19.76 | 6.69 | 5.86 |
| 9 | 10 | 0.80 | 1.32 | 4.5 | 15.76 | 2.76 | 4.6 |
| 10 | 10 | 0.80 | 1.32 | 4.5 | 9.81 | 2.76 | 4.5 |
| | | | | | | | 4.5 |

**Table 2**
Mechanical properties of concrete materials [19].

| Material | Compressive Strength (MPa) | Elasticity Modulus (GPa) | Density (kg/m$^3$) |
|---|---|---|---|
| Arch Concrete | 21 | 22.9 | 2380 |
| Pier Concrete | 22 | 23.4 | 2630 |
| Infill (Concrete) | 12 | 17.3 | 2330 |

accessories of the DCDT sensor and causes that they work precisely.

The DCDT sensors were installed at the middle and the quarter point of main span (Fig. 5).

### 4.2. Accelerometers installation

During the test operations, a one directional accelerometer was measuring the vertical acceleration at the middle of the main span. It is important to observe some main points to install the sensor. For instance the place under the sensor should be clean and smooth enough to cause no deviation in the measured data. The mentioned accelerometer has been installed on a plate at the middle of the span and had the capacity of 5 g.

### 4.3. Load testing: arrangement and operation

For the sake of field load testing, two GT26 locomotives with the weight of 1100 kN have been employed (the locomotives were weighed by the weigh in motion (WIM) system). The load axle's arrangement is displayed in Fig. 6.

As mentioned earlier, passages of the vehicle were occurred in different speeds that were changing between 5 and 58 km/h (there was a speed limitation due to the existence of the curves in the plan). Besides, the sampling frequency was set to 1000 Hz. In Table 3 the test schedules have been expressed.

In the figures beneath (Figs. 7 and 8), the vertical displacements of the middle and the quarter point of main span are presented. In the case of low speed rang (5 km/h) for this test, the load condition was considered as pseudo- static.

**Fig. 5.** DCDT placement on the keystone and the quarter point of span length.

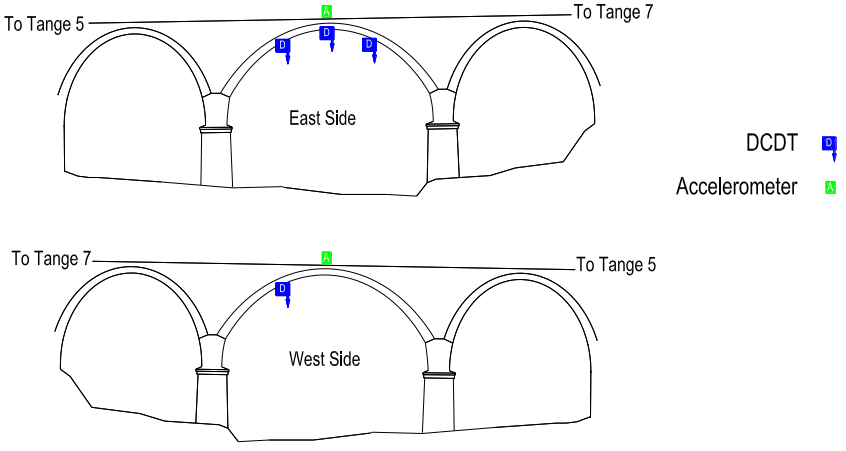


**Fig. 4.** Sensors placement for monitoring.

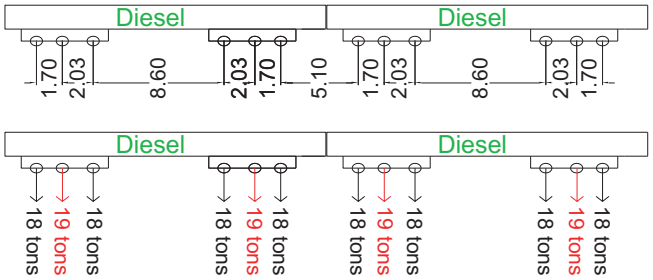


**Fig. 6.** Axle load position and weights.

**Table 3**
Field test schedules.

| Speed (km/h) | Direction | Speed | Direction |
|---|---|---|---|
| 5 | Tange 7–Tange 5 | 52 | Tange 7–Tange 5 |
| 15 | Tange 7–Tange 5 | 29 | Tange 5–Tange 7 |
| 29 | Tange 7–Tange 5 | 50 | Tange 5–Tange 7 |
| 51 | Tange 7–Tange 5 | 58 | Tange 5–Tange 7 |

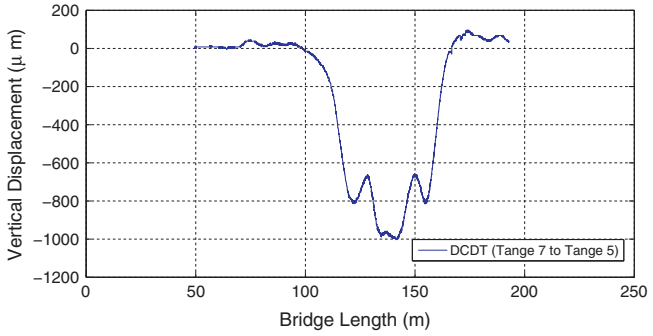


**Fig. 7.** Vertical displacement results at the middle of main arch due to the train passing.

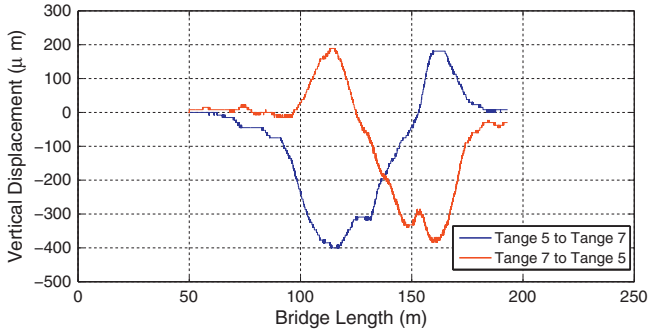


**Fig. 8.** Vertical displacement results at the quarter point of main arch due to the train passing.

## 5. Impact factor calculation

The dynamic impact factor is one of the important parameters in the bridge analysis. Due to the long serviceability period of the bridge and the current condition of this structure, the dynamic impact factor is computed based on the field testing results. It was applied in the assessment of the bridge under the service load (Fig. 16). Besides the control of the structure in the ultimate load calculation was performed. To compute the impact factor, ascending trend in speed rang was studied. These factors were computed as the ratio of dynamic to static displacement in which the bridge displacement during the train passage at the speed of 5 km/h considered as static. Fig. 9 indicates the impact factor vs speed in which the maximum growth in the surveying rang was about 20% ($[(1210-1010)/1010]\times 100 = 19.8\%$). Hence, the value of the calculated dynamic impact factor in the permissible range of train speed is 1.2 while this value is 1.16 in the code [20]. It is worth mentioning that the computed impact factor is exploited in the analysis of the studied bridge.

## 6. RMS calculation of the acceleration

In this research, RMS (Root Mean Square) values for the acceleration at the middle of span (span 7) were calculated, the changes of which in terms of the vehicle speeds could be observed in Fig. 10. Increasing the speed of vehicle from 5 km/h to 60 km/h causes a fivefold growth in the RMS of acceleration. This could be interpreted as the statistical criteria of increasing the vibration level due to the higher speed values.

## 7. Numerical modeling and validation

The three-dimensional model of the bridge has been constructed. The model consists of piers, arch, filler and ballast. Due

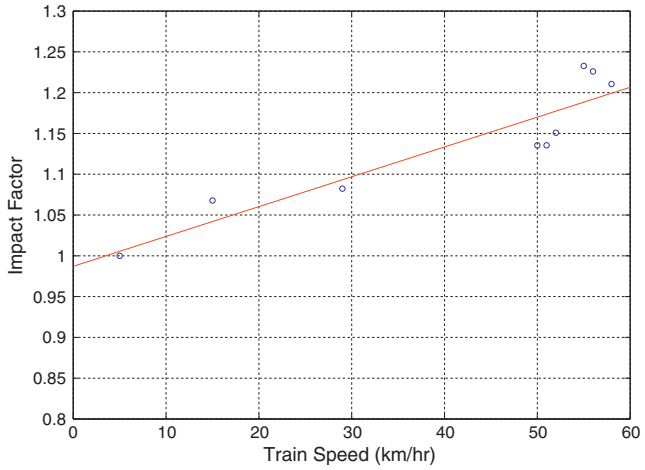


**Fig. 9.** Impact factor due to the train passing with various speeds.

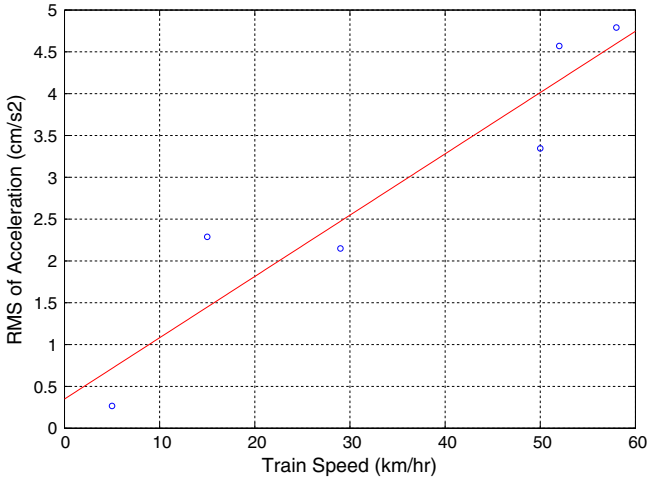


**Fig. 10.** The RMS values of acceleration at the middle of main arch for different speeds.

to the bedrock existence, modeling of the foundation and soil layers have been ignored. Therefore, all degrees of freedom of the piers and main arch at the junction were constrained. All structural components were created through 3D solid (8 nodes) element.

A sensitivity analysis on the mesh dimension has been carried out to observe the effect of maximum mesh dimension on the obtained results. Thus, mesh construction with different maximum dimensions of 70, 50, 40, and 30 cm were performed. By decreasing the mesh dimension from 40 cm to 30 cm, the changes of the model natural frequencies were less than 0.01 Hz, which indicates that 40 cm is a suitable value that could be considered for the mesh dimension. The ultimate created model contains 15,877 elements and 22,674 nodes.

As arches were made of concrete blocks and mortar joints, the following equation could be used to calculate the equivalent compressive strength and elasticity modulus [2].

$$f_k = 0.5 f_b^{0.65} f_m^{0.25} \quad (1)$$

$$E = 5000 + 300 f_b \quad (2)$$

In the above Eqs. (1) and (2), $f_b$ is the compressive strength of the block and $f_m$ is the compressive strength of the mortar. Based on the test experiment [18], the compressive strength of the block and the mortar are 21 MPa and 7 MPa respectively. The equivalent quantity can be observed in Table 4.

In order to considering plasticity effects, the stress–strain diagram of the material, which has been exploited in the bridge analysis, seems like the following curve (Fig. 11).

Fig. 12 shows the ultimate structural model with regard to the meshed parts.

To perceive the accuracy of the model, vertical displacement responses at the middle and the quarter point of main span and under the vehicle (two locomotives) moving speed of 5 km/h have been compared to those obtained from the finite element analysis.

In the Fig. 13 the results of the displacements at the middle of the seventh span, and in the Figs. 14 and 15, the results of the displacements at the quarter point of this span under the passage of two locomotives have been compared. In the comparison procedure both numerical modeling and field testing results were considered. As represented, a reasonable convergence of the

**Table 4**
Equivalent mechanical properties of materials.

| Material | Compressive Strength (MPa) | Elasticity Modulus (GPa) | Poisson Ratio | Density (kg/m$^3$) |
|---|---|---|---|---|
| Arch Concrete | 5.88 | 11.3 | 0.167 | 2380 |
| Pier Concrete | 6.06 | 11.6 | 0.167 | 2630 |

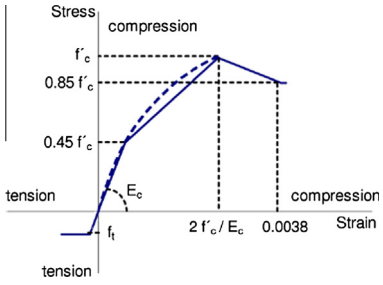


**Fig. 11.** Stress–strain diagram of concrete materials [15].

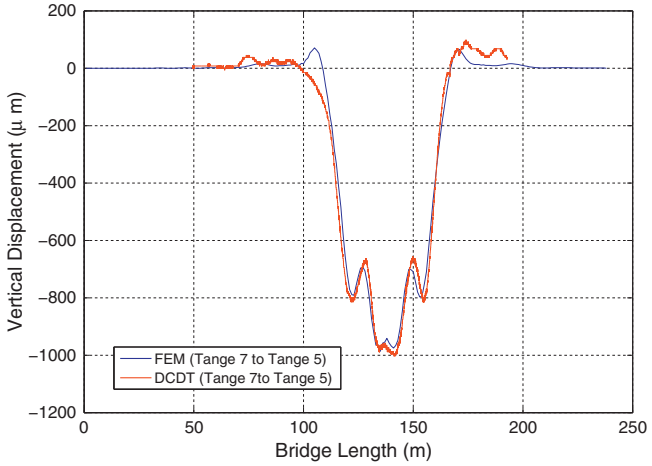


**Fig. 13.** Vertical displacement results at the middle of main arch due to the train passing (Speed: 5 km/h, Direction: Tange 7–Tange 5).

**Fig. 12.** Finite element model of the Saleh Hamid Bridge.

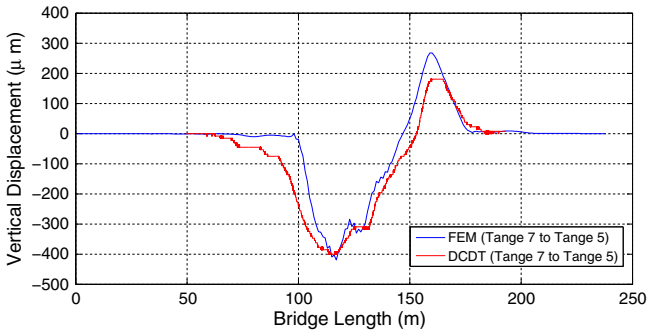


**Fig. 14.** Vertical displacement results at the quarter point of main arch due to the train passing (Speed: 5 km/h, Direction: Tange 7–Tange 5).

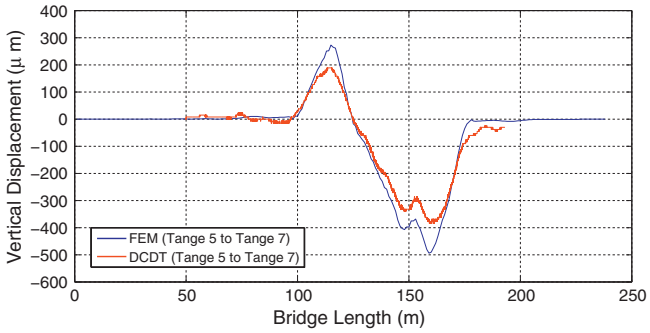


**Fig. 15.** Vertical displacement results at the quarter point of main arch due to the train passing (Speed: 5 km/h, Direction: Tange 5–Tange 7).

numerical modeling and the field testing results, confirms the true applicability of the model for predicting the structural behavior.

## 8. Assessment the potential of allowable axle load Increasing

The formation of four plastic hinges is the most possible fracture mode in the masonry arch bridges [21]. To determine the critical state of the bridge, the standard loading presented in the UIC 776-1 [20] was applied to the middle and the quarter point of span. The standard loading is displayed in Fig. 16. Based on the loading, it is to assess the possibility of axle load increasing from 200 (allowable axle load) to 250 kN.

The loading model and formation of plastic hinges in the created finite element model and the RING software have been presented in Figs. 17 and 18 respectively. These figures are related to the loading applied to the middle of main arch (seventh arch).

Figs. 19 and 20 are related to the loading which was applied on the quarter point of main span. In Figs. 17 and 19, the infill has been hidden to better understanding of the mechanism formation.

The Adequacy factor (the ratio of allowable to current factor) of main span (seventh arch) and side arches (sixth and eight ones) can be observed in Table 5.

The adequacy factors (without considering the partial factors) in Table 5 indicates that the arches to reach the failure mechanism

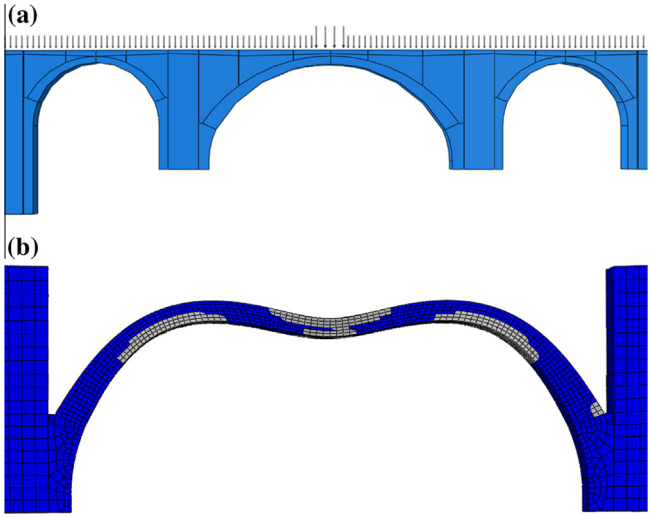


**Fig. 17.** Plastic hinge formation while the middle of main span has been loaded (using the FE method, a and b).

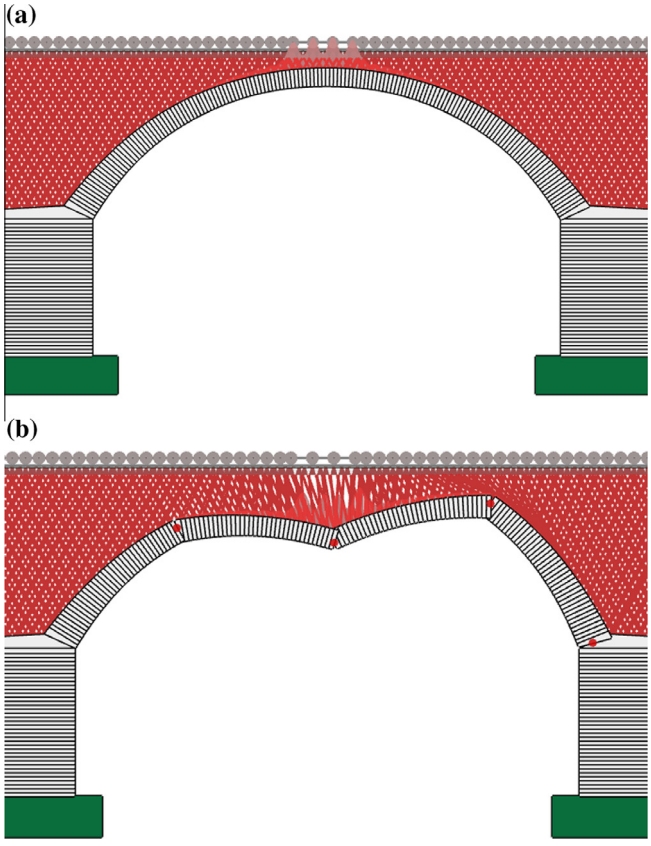


**Fig. 18.** Plastic hinge formation while the middle of main span has been loaded (using the RING software, a and b).

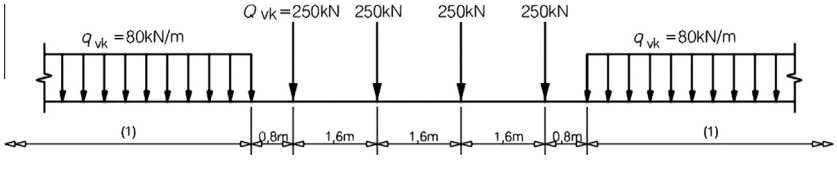


**Fig. 16.** Proposed loading scheme of the UIC 776-1 guideline [20], with the axle load of 250 kN (LM71).

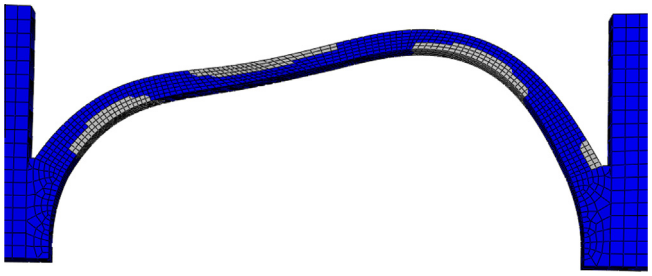

**Fig. 19.** Plastic hinge formation while the quarter point of main span has been loaded (using the FE method).

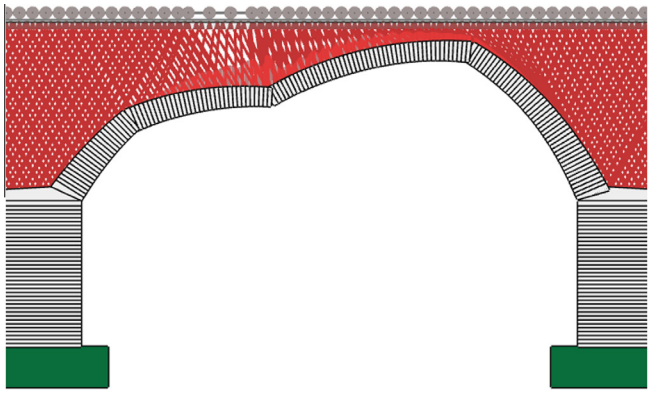

**Fig. 20.** Plastic hinge formation while the quarter point of main span has been loaded (using the RING software).

**Table 5**
Adequacy Factors of the Bridge.

| Arch Number | Span Length | RING Software | | FE Method | |
|---|---|---|---|---|---|
| | | @ One Fourth | @ Middle | @ One Fourth | @ Middle |
| 7 | 40 | 6 | 5.2 | 6.26 | 5.24 |
| 6 and 8 | 21 | 8.2 | 7.8 | 8.68 | 8.02 |

**Table 6**
Adequacy Factors of the Bridge by Considering the Partial Factors.

| Arch Number | Span Length | RING Software | | FE Method | |
|---|---|---|---|---|---|
| | | @ the quarter point | @ the Middle | @ the quarter point | @ the Middle |
| 7 | 40 | 1.38 | 1.25 | 1.43 | 1.31 |
| 6 and 8 | 21 | 2.58 | 1.97 | 2.66 | 2.05 |

are able to withstand the several times more loading rate than the standard ones.

However, to control the bridge in ultimate limit state, the partial factors need to be considered according to the codes. Hence, based on the UIC778-3 [2], EN 1990:2002+A1 [22] and EN 1996-1-1 [23], the partial factors for permanent loads is 1.35, for service load is 1.45, and for material strength is 2.5. According to the field testing, the impact factor was considered as 1.2. By considering the mentioned factor, the adequacy factors in the arches are as following (Table 6).

According to the illustrated results in the above table, the bridge could be in service for the current standard loading that makes it possible to increase the axle load up to 250 kN.

## 9. Controlling the bridge in serviceability limit state

One of the main methods to evaluate the masonry arch bridges is controlling this kind of structures in serviceability limit state that are based on the eccentricity limit state and controlling the allowable compressive stresses. According to the BD 91/04 code [24], in the serviceability limit state, under the loading condition of D + 1.2L, the following criteria need to be satisfied. It is worth mentioning that in calculation of service load, the dynamic impact factor has been considered (This factor was obtained according to the field testing results and the speed limit up to 60 km/h).

$$e < 0.25\ h \tag{3}$$

$$\sigma_{compression} < 0.4 f_k \tag{4}$$

e is the load eccentricity, H is the considered height and $f_k$ is the compressive strength of materials.

Based on the above equations, the values of compressive stresses, allowable compressive stresses and load eccentricities under current standard loading (Fig. 16) in different spans are shown in Table 7.

As it can be observed in the Table 7, all values of compressive stresses are less than the allowable compressive stress and the minimum adequacy factor of compressive stress is 1.05. The values of load eccentricity in all conditions are less than 0.25 and within the allowable limit. The minimum adequacy factor for eccentricity is 1.19. Consequently, based the mentioned limit states, the bridge has enough capacity to resist the current standard service loading (Fig. 16) that shows the possibility of axle load enhancement up to 250 kN.

## 10. Discussion and conclusions

The main objective of this research project was the evaluation of a masonry arch bridge under the standard loading (Fig. 16) to assess the possibility of load increasing.

**Table 7**
Compressive strength and allowable compressive strength (the height and load eccentricities have been considered).

| Nth Span | Location | Top | Stress/(Mpa) | | h (mm) | e (mm) | e/h | Exerted < Allowable |
|---|---|---|---|---|---|---|---|---|
| | | Bottom | Allowable | Exerted | | | | |
| 6th span | Middle span | Top. Fiber | −2.35 | −2.10 | 1000 | 207.55 | 0.21 | OK |
| | | Bot. Fiber | −2.35 | 0.23 | | | | |
| | Quarter point of span | Top. Fiber | −2.35 | −0.59 | 1230 | 57.46 | 0.05 | OK |
| | | Bot. Fiber | −2.35 | −1.05 | | | | |
| 7th span | Middle span | Top. Fiber | −2.35 | −2.24 | 1400 | 189.20 | 0.14 | OK |
| | | Bot. Fiber | −2.35 | −0.23 | | | | |
| | Quarter point of span | Top. Fiber | −2.35 | −0.89 | 1680 | 69.99 | 0.04 | OK |
| | | Bot. Fiber | −2.35 | −1.48 | | | | |
| 8th span | Middle span | Top. Fiber | −2.35 | −1.95 | 1000 | 211.45 | 0.21 | OK |
| | | Bot. Fiber | −2.35 | 0.23 | | | | |
| | Quarter point of span | Top. Fiber | −2.35 | −0.49 | 1230 | 68.59 | 0.06 | OK |
| | | Bot. Fiber | −2.35 | −0.99 | | | | |

For this aim, the field load testing of the Saleh-Hamid Bridge, which is about 80 years old, under the passage of two locomotives with different speeds (5–60 km/h) was performed. Through the bridge instrumentation, vertical displacements and acceleration in different locations (at the middle and the quarter point of span) were recorded and dynamic impact factor was computed. In order to evaluate the possibility of axle load increasing, a 3D finite element model was created. Material properties were obtained by taking advantage of strength of materials experiments. In order to validate the numerical modeling, the bridge displacements at the middle and the quarter point of span have been compared to those from the FE analysis. There is a good agreement between the results of the field load testing and the numerical analysis and the created model was verified accordingly.

Then, the capacity assessment of the bridge was performed based on the following methods:

1) Ultimate load calculation with the updated FEM (based on the four plastic hinges mechanism and disregarding the partial factors for load and material).
2) Ultimate load calculation with the RING [18] software (Disregarding the partial factors for load and material).
3) Two aforementioned items while considering the partial factors for load and material, and also considering the impact factor.
4) Using the updated FEM for controlling the bridge in serviceability limit state.

To assess the current capacity of the bridge, the four plastic hinges mechanism method was used. The results of the FEM and the RING modeling for the standard loading (Fig. 16) indicate the value 1.25 (Table 6) as the minimum coefficient for bridge capacity with considering the partial factors.

Based on the eccentricity criteria and the allowable compressive stress, the bridge adequacy factors were computed as 1.19 and 1.05 respectively. This coefficient indicates that the studied bridge can still be in service. Moreover, the evaluation shows that the bridge has the capacity for carrying axle loads up to 250 kN.

## Acknowledgement

The author would like to thank the financial support of Iranian Railway Organization under project number S/5547 with industrial project cooperation office of Iran University of Science and Technology.

## References

[1] P.J. Fanning, T.E. Boothby, Three-dimensional modeling and full scale testing of stone arch bridges, Comput. Struct. 79 (2001) 2645–2662.
[2] UIC Code 778-3R, Recommendations for the Assessment of the Load Carrying Capacity of Existing Masonry and Mass-concrete Arch Bridges, second ed., 2011.
[3] SB4.7, Structural Assessment of Masonry Arch Bridges, Background Document, Prepared by Sustainable Bridges- A Project within EU FP6, 2007. Available from: www.sustainablebridges.net (cited 30 November 2007).
[4] T. Boothby, S. Atamturktur, A guide for the finite element analysis of historic load bearing masonry structures, in: Proceedings of the 10th North American Masonry Conference, Missouri (United States of America), 2007.
[5] L. Fryba, M. Pirner, Load tests and modal analysis of bridges, Eng. Struct. 23 (2001) 102–109.
[6] M.S. Marefat, E. Ghahremani, Sh. Ataei, Load test of a plain concrete arch railway bridge of 20-m span, Constr. Build. Mater. 18 (2004) 661–667.
[7] Y. Robert-Nicoud, B. Raphael, O. Burdet, I.F.C. Smith, Model identification of bridges using measurement data, Comput.-Aided Civ. Infrastruct. 20 (2005) 118–131.
[8] B. Ozden, K. Ozakgul, O. Tezer, Assessment of a concrete arch bridge using static and dynamic load tests, Struct. Eng. Mech. 41 (1) (2012) 83–94.
[9] A.J. Carr, D.V. Jauregui, B. Riveiro, P. Arias, J. Armesto, Structural evaluation of historic masonry arch bridges based on first hinge formation, Constr. Build. Mater. 47 (2013) 569–578.
[10] E. Reccia, G. Milani, A. Cecchi, A. Tralli, Full 3D homogenization approach to investigate the behavior of masonry arch bridges: the Venice trans-lagoon railway bridge, Constr. Build. Mater. 66 (2014) 567–586.
[11] J. Heyman, The Masonry Arch, Ellis Horwood Limited, Chichester (England), 1982.
[12] W.J. Harvey, Application of the mechanism analysis to masonry arches, Struct. Eng. 66 (1988) 77–84.
[13] C. Costa, D. Ribeiro, P. Jorge, R. Silva, R. Calcada, A. Arede, Calibration of the numerical model of a short-span masonry railway bridge based on experimental modal parameters, Procedia Eng. 114 (2015) 846–853.
[14] A. Cavicchi, L. Gambarotta, Two-dimensional finite element upper bound limit analysis of masonry bridges, Comput. Struct. 84 (2006) 2316–2328.
[15] K.H. Ng, C.A. Fairfield, Modifying the mechanism method of masonry arch bridge analysis, Constr. Build. Mater. 18 (2004) 91–97.
[16] A. Brencich, D. Sabia, Experimental identification of a multi-span masonry bridge: the Tanaro Bridge, Constr. Build. Mater. 22 (2008) 2087–2099.
[17] ABAQUS Inc, ABAQUS Version 6.10.1. Analysis User's Manual, 2010.
[18] Limit State Ltd., Ring 3.1 software.
[19] Iranian Railways, Experimental Studies on Strength of Materials (Bridge Km-556+400, Lorestan, Iran), 2006.
[20] UIC Code 776-1, Loads to be Considered in Railway Bridge Design, fifth ed., 2006.
[21] A. Audenaert, H. Peremans, G. Reniers, An analytical model to determine the ultimate load on masonry arch bridges, J. Eng. Math. 59 (2007) 323–336.
[22] EN 1990:2002: Eurocodes – Basis of Structural Design – Part 2: National Annex to EN, 1990:2002.
[23] EN 1996-1-1:2005, Eurocode 6 – Design of Masonry Structures – Part 1-1: General Rules for Reinforced and Unreinforced Masonry Structure, 2006.
[24] Code BD 91/04, Design Manual for Roads and Bridges, Un-Reinforced Masonry Arch Bridges, 2004.